Semiconductor Physics, Quantum Electronics & Optoelectronics. 2004. V. 7, N 4. P. 333-338.

PACS: 63.2D.-e, 72.10.Di, 73.21.Cd

Effects of LO-phonon confinement on electron mobility in GaAs-$Al_{0.45}Ga_{0.55}As$ superlattice

D. Abouelaoualim

L.P.S.C.M, Physics Department, Faculty of Sciences-Semlalia
BP: 2390, 40000, Marrakech, Morocco
E-mail: abouelaoualim_d@hotmail.com

Abstract. The parallel and perpendicular electron mobilities in a GaAs-$Al_{0.45}Ga_{0.55}As$ superlattice have been calculated. The scattering of electrons by confined longitudinal optical phonons was taken into account. Using the quantum treatment, we offered the new wavefunction of electron miniband conduction in the superlattice as well as reformulation of the slab model for confined LO-phonon modes. An expression for the relaxation time was obtained. Our results show that the relaxation time depends significantly on the total energy of electrons. The effect of the band nonparabolicity on the relaxation time was analyzed. At 300 K, the calculated results reveal that the electron mobility is enhanced when the well width in the superlattice is equal to 45 Å.

Keywords: phonon confinement, electron mobility, superlattice.

Manuscript received 20.07.04; revised manuscript received 23.11.04; accepted for publication 16.12.04.

1. Introduction

Recently there has been much interest in the study of electron–phonon interaction in III-V semiconductor quantum wells (QWs) and superlattices (SLs) [1-3]. It is because of the phonon scattering determines electron transport properties at the room temperature and high electric fields as well as at low temperatures. For instance, cooling the photoexcited carriers, carrier tunnelling, and mobility in high-speed heterostructure devices are primarily governed by the scattering of electrons by polar optical phonons. Some results in Raman scattering, cyclotron-resonance and magnetophonon-resonance measurements show the dominance of electron interaction with LO-phonons and reveal important information about the vibration modes in the layers forming SL [4-10]. The electron – LO-phonon interaction was found to be strongly dependent on both the geometrical shape and the parameters of the constituent materials [11-12]. The polaron effect in heterostructures of a small thickness is, however, quite different from that in bulk materials. Several models have been proposed to describe the electron – confined LO-phonon interaction in superlattices. Dielectric continuum models [13-14], microscopic lattice dynamical models [17-19], or the slab model [20-21]. Several theoretical studies have been already reported on calculations of the relaxation time caused by the carrier scattering due to interaction with optical phonons in semiconductor heterostuctures, the cases of single or multiple quantum wells being treated [22-25].

In this work, we have investigated the influence of sub-band nonparabolicity on the relaxation time due to electron – confined LO-phonon interaction calculated using a quantum formalism. We study the dispersion of the mobility. The organization of the present paper is as follows: Section II summarizes the theoretical framework used in the calculations, while Section III contains the discussion of numerical results presented graphically, and brief conclusion is given.

2. Theoretical model

2.1. Miniband structure and envelope wavefunctions

Using the effective mass Hamiltonian and the transfer matrix method, the total energy of electron associated to the first miniband and the analytically exact normalized wavefunction [26] can be written as follows:

$$\varepsilon_{\xi} = \frac{\hbar^2 k_{\perp}^2}{2m_w^{*2}} + E_1^* - \frac{\Delta_1}{2}\cos(k_z l). \qquad (1)$$

$$\Psi_w(z) = \frac{e^{-ik\frac{1}{2}}e^{ink_z l}}{\sqrt{N}}\left\{b_2 e^{ik(z-(n-\frac{1}{2}))} + \beta e^{-ik(z-(n-\frac{1}{2}))}\right\},$$

$$-L + l_b < z - nl < l_b. \qquad (2)$$

$$\Psi_b(z)=\frac{e^{-ik\frac{1}{2}}e^{ink_z l}}{\sqrt{N}}\begin{Bmatrix} p\cosh[\rho(z-nl+l_b)]+\\ +q\sinh[\rho(z-nl+l_b)]\end{Bmatrix},$$

$$-l_b < z-nl < l_b\,. \qquad (3)$$

$$\hbar^2k^2=2m_w^*E\,, \qquad h^2\rho^2=2m_b^*(V_b-E)\,,$$

$$\lambda=m_w^*/m_b^*, \qquad L=l_b+l_w\,. \qquad (4)$$

$$x=kl_w\,, \qquad y=\rho l_b\,,$$

$$\beta=\sin(x)\cosh(y)-K^-\cos(x)\sinh(y)-\sin(k_z l). \qquad (5)$$

$$p=b_2e^{ix/2}+\beta^-e^{-ix/2}\,,$$

$$q=\frac{ik}{\lambda\rho}\left(e^{ix/2}-\beta^-e^{-ix/2}\right). \qquad (6)$$

$$k^{\pm}=\frac{1}{2}\left(\frac{\lambda\rho}{k}\pm\frac{k}{\lambda\rho}\right), \qquad b_2=k^+\sinh(y), \qquad (7)$$

$$N=A'\left(b_2^2+(\beta^-)^2\right)+B'\beta^-\,. \qquad (8)$$

$$\Pi^{\mp}=\left(\frac{2k}{\lambda\rho}\right)K^{\pm}, \qquad (9)$$

$$A'=l_w+\begin{pmatrix} l_b\left[\frac{\Pi^-}{2}+\Pi^-\frac{\sinh(2y)}{4y}\right]\cos(x)+\\ +\left[\frac{1}{k}-\frac{k}{\lambda\rho}\frac{\cosh(2y)-1}{2\rho}\right]\sin(x)\end{pmatrix}, \qquad (10)$$

$$B'=2b_2\begin{Bmatrix} L_b\left[\Pi^+/2+\Pi^-(\sinh(2L_b\rho)/4L_b\rho)\right]\cos(kL_w)+\\ +\left[\left(1-\cosh(2L_b\rho)/2\lambda\rho^2\right)k+1/k\right]\sin(kL_w)\end{Bmatrix}. \qquad (11)$$

2.2. Relaxation time

The Hamiltonian of electron-phonon interaction in low dimensional systems depends on the specific phonon spectra in the system and is different from the Fröhlich Hamiltonian for bulk phonons. The macroscopic dielectric continuum model [27-30] gives the functional form of the interface modes, confined and half-space LO modes. The electron – confined LO-phonon interaction Hamiltonian as derived from Fröhlich interaction is given by [31, 32]

$$H_{e\text{-}p}=\lambda\sum_{q_\perp,n\alpha=\pm}\sum e^{iq_\perp r}H(z)t_{n\alpha}(q_\perp)u_{n\alpha}(z)\times \qquad (12)$$
$$\times\left[a_{n\alpha}(q_\perp)+a^+{}_{n\alpha}(-q_\perp)\right]$$

where $a(q)$ and $a^+(q)$ are the creation and annihilation operators for bulk phonons in the q mode, "–" and "+" signs denote even and odd confined phonon modes, and n is the miniband index, while the coupling constant

$$\lambda^2=iC_\mu/\sqrt{Vq} \qquad (13)$$

where V is the volume.

From [33], C can be written explicitly as

$$C=\left[\frac{e^2\hbar\omega_{LO}}{2\varepsilon_0}\left(\frac{1}{\varepsilon(\infty)}-\frac{1}{\varepsilon(0)}\right)\right]^{\frac{1}{2}} \qquad (14)$$

where $\hbar\omega_{\rm LO}$ is the energy of the LO-phonon in the n-th miniband, $\varepsilon(\infty)$ and $\varepsilon(0)$ are the optical and static dielectric constants, respectively, Ω is the volume, and e is the electronic charge. For the slab model [27, 34] $u_{n\alpha}(z)$ are defined as

$$u_{n+}(z)=\cos(n\pi z/L_w)\,, \qquad n=1,3,5,\ldots \qquad (15)$$

$$u_{n-}(z)=\sin(n\pi z/L_w)\,, \qquad n=2,4,6,\ldots \qquad (16)$$

$t_{n\alpha}$ is given by

$$t_{n\alpha}=\frac{1}{[q_\perp^2+(n\pi/L_w)^2]^{1/2}}\,, \qquad n=1,2,3,\ldots \qquad (17)$$

Finally,

$$H(z)=\begin{cases}1, & \text{if } -w\le z\le w\\ 0, & \text{otherwise}\end{cases}. \qquad (18)$$

The scattering rate $w_{i\to f}$ appearing is obtained from the Fermi Golden Rule

$$W_{i\to f}(k)=\frac{2\pi}{\hbar}\sum_f\left|\left\langle\xi_f\left|H_{e-p}\right|\xi_i\right\rangle\right|^2. \qquad (19)$$

Evaluating the matrix element in (21) with the Hamiltonian given by (14), we obtain

$$W_{i\to f}=\frac{\pi}{2\pi V\hbar}(N_{\rm LO}+\frac{1}{2}\pm\frac{1}{2})\frac{e^2\hbar\omega_{\rm LO}}{q_\pm}\times$$
$$\times\left(\frac{1}{\varepsilon(\infty)}-\frac{1}{\varepsilon(0)}\right)\delta(U^\pm)I(k_z^i,k_z^f,q_\perp) \qquad (20)$$

where

$$I_n(k_z^i,k_z^f,q_\perp)=\sum_{q_\perp}\sum_{n,\alpha}\left|G_{n,\alpha}^{i\to f}(k_z^i,k_z^f)\right|^2\times$$
$$\times\left|t_{n,\alpha}(q_\perp)\right|^2. \qquad (21)$$

The δ-function represents the energy conservation quantity

$$\delta(U^\pm)=\delta\left(\frac{\hbar^2}{2m^*}({k_\perp^i}^2-{k_\perp^f}^2)+E_{k_z^f}-E_{k_z^i}\pm\hbar\omega_{\rm LO}(q_\pm)\right),$$

"±" stands for absorption and emission processes. For optical phonon scattering

$$q_\pm^2={k_\perp^i}^2-{k_\perp^f}^2-2k_\perp^ik_\perp^f\cos\theta+(k_z^i-k_z^f\mp G)^2=cte\,. \qquad (22)$$

G is the reciprocal lattice vector of SL. $N_{\rm LO}$ is the LO-phonon occupation number defined as:

$$N_{\rm LO}=(\exp\frac{\hbar\omega_{\rm LO}}{k_{\rm B}T}-1)^{-1}. \qquad (23)$$

$G_{n,\alpha}^{i\to f}(k_z^i,k_z^f)$ is the overlap integral of the electron wavefunction and the *z*-dependent of the electron – confined-phonon Hamiltonian

$$G_{n,\alpha}^{i\to f}(k_z^i,k_z^f)=\int_{-l/2}^{l/2}\psi_f^*(z)u_{n,\alpha}\psi_i^*(z)\mathrm{d}z \qquad (24)$$

where ψ_i, ψ_f are the electron envelope miniband wavefunctions in the initial and final states, respectively [31]. L is the period SL; $L=L_w+L_b$. At $U^{\pm}=0$, $k_\perp^f$ and $k_\perp^i$ terms must equal. We define a coordinates system and general lines of summation over k_f states:

$$\sum_{k_f}=\frac{V}{(2\pi)^3}\int_0^\infty k_\perp^f\mathrm{d}k_\perp^f\int_0^{2\pi}\mathrm{d}\theta_f\int_{-\frac{\pi}{L}}^{\frac{\pi}{L}}\mathrm{d}k_z^f \qquad (25)$$

where $k_\perp^f$, θ are the polar coordinates in the planes normal to k_z^f defined earlier.

We use also the following Jacobian

$$\frac{\partial U^{\pm}}{\partial k_\perp^f}=\frac{\hbar^2}{m^*}k_\perp. \qquad (26)$$

Using relations (20), (24), (26), (27) and (28), the expression for the scattering time due to the interaction electron – confined-phonon τ^{-1} is calculated by applying the first-order perturbation theory:

$$\tau_{\mathrm{op}}^{-1}=\frac{1}{\tau_0 k_\perp}\int_0^{2\pi}\mathrm{d}\theta\left\{\int_{\gamma+}\frac{I_{n,\alpha}^{+}(k_z^i,k_z^f,q_\perp)\left[N_{\mathrm{LO}}(\omega)+1\right]\mathrm{d}k_z^f}{q_+^2}+\int_{\gamma^-}\frac{I_{n,\alpha}^{-}(k_z^i,k_z^f,q_\perp)\left[N_{\mathrm{LO}}(\omega)+1\right]\mathrm{d}k_z^f}{q_-^2}\right\}, \qquad (27)$$

$\gamma^{\pm}$ is the integration domain over k_z^f represented in Fig. 1.

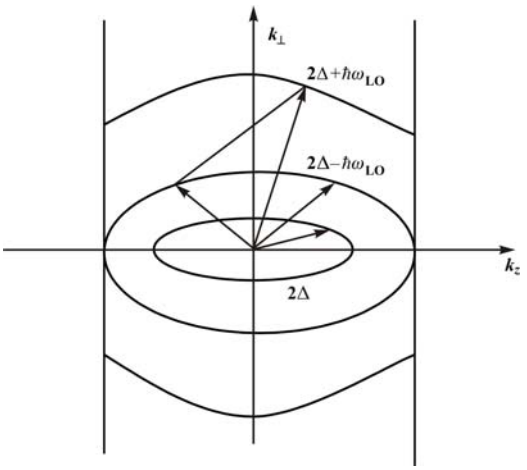

Fig. 1. Representation of constant-energy lines $\varepsilon_\xi(K)=\mathrm{const}$ in plan ($k_\perp$, k_z). The difference is constant, $\hbar\omega_{\mathrm{LO}}$. Two examples are drawn $2\Delta+\hbar\omega_{\mathrm{LO}}$ and $2\Delta-\hbar\omega_{\mathrm{LO}}$.

2.3. Electron mobility

The electron mobility is given by the following expression:

$$\mu_{\eta\nu'}=\frac{2}{N}\frac{e}{\Omega}\sum_\xi\left(-\frac{\partial f}{\partial\varepsilon_\xi}\right)v_{\eta\xi}v_{\nu\xi}\tau(\varepsilon_\xi). \qquad (28)$$

Here, $f(\varepsilon_\xi)$ is the distribution function for the electron in SL and N is the concentration of electrons in the first miniband of the superlattice. For the case of non-degenerated statistics for the electron, $\Delta >> k_{\mathrm{B}}T$, in a accord with the Maxwellian distribution. Using the equation (27), the parallel and perpendicular electron mobilities can be represented as

$$\mu_{zz}=\frac{k_{\mathrm{B}}T}{4\hbar}\frac{el\Delta}{N}\sum_{k_\perp k_z}\sin^2(k_z l)e^{-\beta(\varepsilon_\xi-\mu)}\tau(\varepsilon_\xi), \qquad (29)$$

$$\mu_\perp=\frac{k_{\mathrm{B}}T}{4\hbar}\frac{el\Delta}{N}\sum_{k_\perp k_z}\left(\frac{\hbar k}{m_w^*}\right)^2 e^{-\beta(\varepsilon_\zeta-\mu)}\tau(\varepsilon_\zeta). \qquad (30)$$

2.4. Nonparabolicity effect

According to the Kane model [35-37], the eigenfunctions of the Hamiltonian in the direction of the superlattice (with $k_x=k_y=0$) associated to a conduction band electron [38, 39] with an energy $0<E<V_b$ are solutions of the Schrödinger equation [40]:

$$\left(\hbar^2 a_2\frac{\partial^2}{\partial z^2}+\hbar^4 a_4\frac{\partial^4}{\partial z^4}\right)y(z)+ +\left(E-V(z)\right)y(z)=0, \qquad (31)$$

$$a_2=\frac{1}{2m^*(z)},\qquad a_4=\frac{1}{E_g}\left(\frac{1}{2m^*}-\frac{1}{2m_0}\right). \qquad (32)$$

The corrective term reflects the nonparabolicity effect (via a_4). Integration of Eq. (31) through an interface of a small arbitrary thickness provides the new boundary conditions:

$$a_{2,w}\psi_w'+a_{4,w}\hbar^2\psi_w'''=a_{2,b}\psi_b'+a_{4,b}\hbar^2\psi_b'''. \qquad (33)$$

This expression that ensures the continuity of the local current density generalizes that of [41, 43] where $a_4=0$ in the case of nonparabolicity, the wavefunctions corresponding to the new condition (31) generalizes those where the continuity of $\frac{1}{m^*}\frac{\mathrm{d}\Psi}{\mathrm{d}z}$ is used. As the latter Hamiltonian without parabolicity, the wavefunctions are given in the *n*-th well and barrier by Eqs (2), (3). Due to the new conditions (31), when deriving the wavefunction the analysis of the preceding sections can be used with λ replaced by μ that we define as follows. From Eq. (31), expressions of *k*, ρ and μ are given by:

$$\hbar^2 k^2 = 4m_w^* E_{w,\max}\left\{1-\sqrt{1-\frac{E}{E_{w,\max}}}\right\},$$

$$E_{w,\max}=\left(\frac{a_2^2}{4a_4}\right)_w; \qquad (34)$$

$$\hbar^2\rho^2 = 4\,m_b^*\,(E_{b,\max}-V_0)\left\{-1+\sqrt{1+\frac{V_0-E}{E_{b,\max}-V_0}}\right\},$$

$$E_{b,\max}=\left(\frac{a_2^2}{4a_4}\right)_b; \qquad (35)$$

$$\mu=\frac{a_{2,b}+\hbar^2\rho^2 a_{4,b}}{a_{2,w}-\hbar^2 k^2 a_{4,w}}. \qquad (36)$$

When introducing the new expressions of wavevectors k and ρ in Eqs (34) and (35), we obtained the new expressions for the dispersion relation and wavefunctions inside the barrier and the wells of SL, by continuation those of the relaxation times and mobility.

If the effect of the nonparabolicity becomes negligible ($a_4 = 0$), $\mu \to \lambda = \frac{m_w^*}{m_b^*}$, defined in the parabolic case. Eqs (34), (35) allow an explicit relationship of ρ in relation with k. For $E_{\max}^b - V_b = E_{\max}^w$ (i.e. $k_0^2 = \lambda\rho_0^2$) insignificant values of ρ and k, we find the parabolic case given by relation (4).

3. Numerical results and discussion

For numerical computation, we have chosen the $GaAs-Ga_{1-x}Al_xAs$ with $x = 0.45$ as a superlattice. The parameters pertaining to the system are: $m_w^* = 0.067m_0$, $m_b^* = 0.104m_0$, where m_0 is the free electron mass. The dielectric constant in the wells is taken equal to that in barrier: $\varepsilon_d = 12.8$, $\varepsilon_\infty = 10.9$, $l_w = 108$ Å, $l_b = 38$ Å, $V_b = 495$ meV. The energy of the bulk GaAs LO-phonon $\hbar\omega_{LO} = 36.8$ meV, the static and high frequency dielectric constants for GaAs: $\varepsilon_s = 12.35$ and $\varepsilon_\infty = 10.48$.

When solving numerically, a partial differential equation for the phonon generation rate with the value $x = 0.45$ was defined as:

$$\frac{\partial N_q}{\partial t}=\frac{2\pi}{\hbar}(N_q+1)\sum_k\left|M_q\right|^2 f(K,t)\times$$
$$\times\left[1-f(K-q,t)\right]\delta(\varepsilon_{\xi K-q}-\varepsilon_{\xi K}+E_{LO})-$$
$$-\frac{2\pi}{\hbar}N_q\sum_k\left|M_q\right|^2 f(K,t)[1-f(K+q,t)]\times \qquad (37)$$
$$\times\delta(\varepsilon_{\xi K-q}-\varepsilon_{\xi K}+E_{LO})-\frac{N_q}{\tau_q}$$

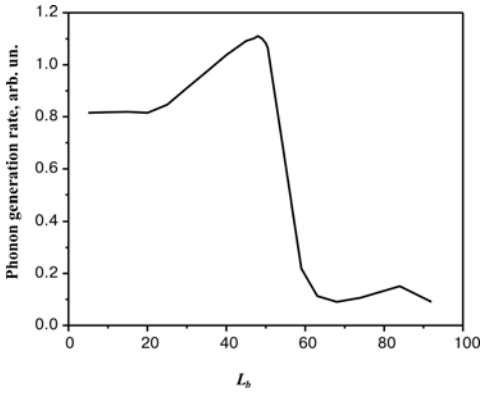

Fig. 2. Representation of the phonon generation rate versus L_b.

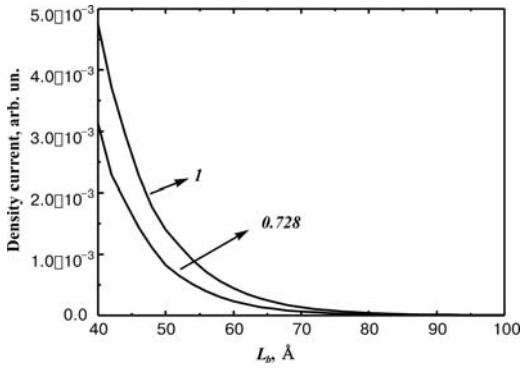

Fig. 3. Density current versus L_b for two different values of rapport masses.

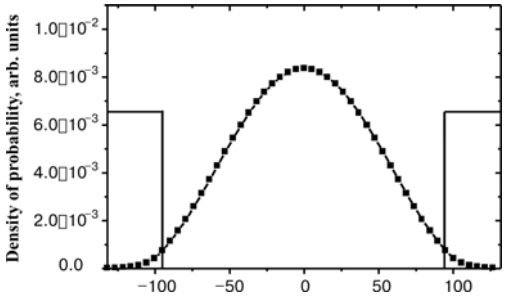

Fig. 4. Density of probability associated to an electron of the first miniband in the approximation of the liaisons fortes. Links pace of potential is to indicate the positions of the barrier and well of superlattice.

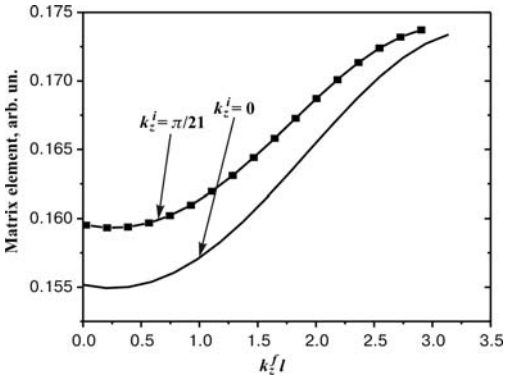

Fig. 5. Plots of the matrix element as $k_z^f l$ for different k_z^i.

where $|M_q|^2$ is the electron – confined LO-phonon interaction matrix element squared, E_{LO} and τ_q are the LO-phonon energy and lifetime, respectively (see Fig. 2). We observe a strong barrier width L_b dependence of the phonon generation rate. When the barrier width L_b increases, the phonon generation rate increases reaching a maximum, so much as L_b is lower than L_{bc} critical value. We deduce the existence of a critical value L_{bc} which the LO-phonon transit from propagation to confinement. The variation of the current density with barrier width is plotted in Fig. 3. We further notice that the current density decreases with increasing barrier width. Accordingly, the tunnelling probability behaves. In Fig. 4, we present the density probability associated to an electron in conduction miniband. We see that its maximum is located in the middle of superlattice quantum wells, so the major electrons are found. The interaction electron – LO-phonon is strong in the wells of superlattice but weak inside the barriers. Another quantity that influences the interaction electron – LO-phonon is the overlap integral given by Eq. (24). It is plotted for some value of final wavevector for several values of the initial wavevector, see Fig. 5. Thus, the final wavevector k_z^f is larger while the quantity $G_{n,\alpha}^{i\to f}(k_z^i, k_z^f)$ presents larger overlap integrals for increasing scattering rates. Fig. 6 illustrates the relaxation time due to the interaction electron – confined LO-phonon confined as function of the total energy ε_ξ for the case of a parabolic miniband:

- for the total energy ε_ξ from the interval $2\Delta - \hbar\omega_{LO} < \varepsilon_\xi < \hbar\omega_{LO}$, we remark the linear increase of the relaxation time, which is interpreted as the increase of the transition probability;
- if $\hbar\omega_{LO} < \varepsilon_\xi < 2\Delta + \hbar\omega_{LO}$, the relaxation time decreases, this has been commented above as the transition limited in

$$I^{\pm}(-\frac{\pi}{L} < k_z^f < \frac{\pi}{L}) \qquad (38)$$

and for the larger energy miniband the electron couples weakly to the phonon (see Fig. 7).

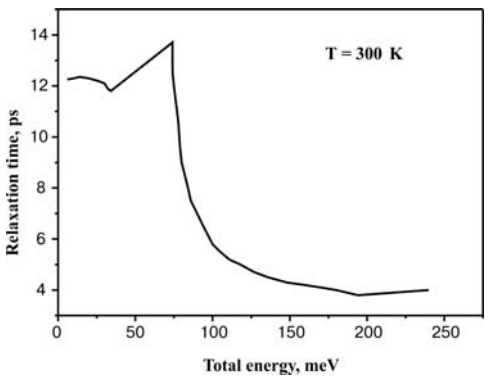

Fig. 6. Scattering times in GaAs-$Al_xGa_{1-x}As$ superlattice as function of the total energy for $k_z^i = \pi/21$.

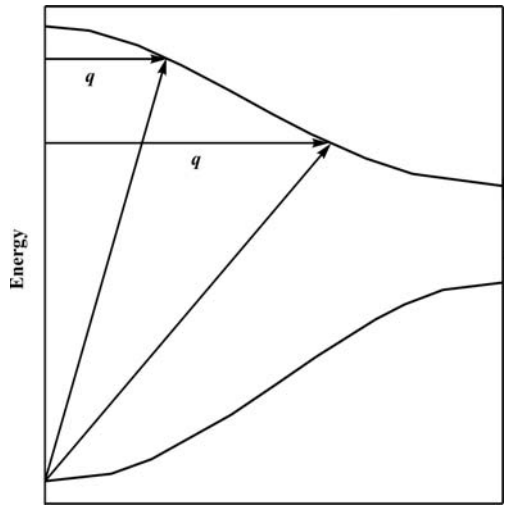

Fig. 7. Schema diagram of phonon wavevector.

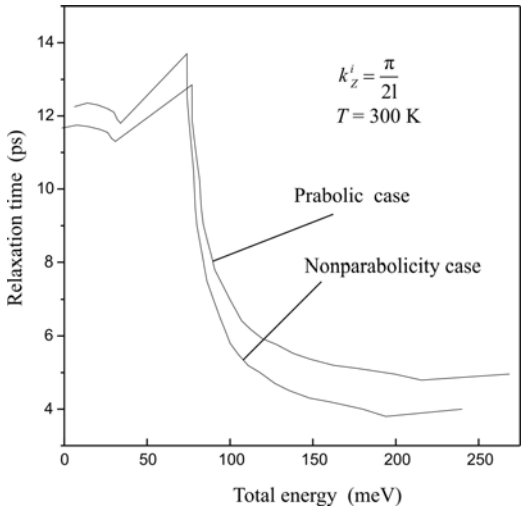

Fig. 8. Relaxation times in GaAs-$Al_{0.45}$ $Ga_{0.55}$ As superlattice as function of the total energy for the case parabolic and nonparabolicity band.

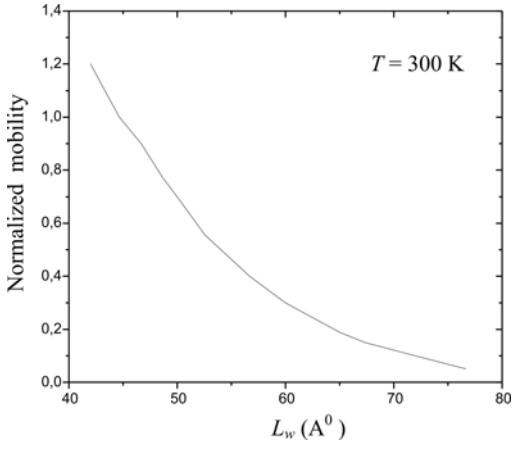

Fig. 9. Electron mobility dependence for several period of GaAs-$Al_{0.45}Ga_{0.55}As$ superlattice.

Fig. 8 displays a comparison between the parallel relaxation times with or without the effect nonparabolicity band. We found this effect to be extremely small for the small energies. This result can be explained by the nonparabolicity effects on the position and widths of minibands. The final results concern the electron mobility limited by polar optical phonon scattering at 300 K. The electron mobility μ_{zz} is normalized to μ_{3d} of the bulk GaAs. In Fig. 9, we represent the dispersion of mobility with the superlattice well width L_w. Our results show that μ_{zz} exponentially decreases with L_w. It is clearly seen from Eq. (29). The miniband width factor Δ contributes and depends on L_w. At $L_w < 45$ Å

$$\frac{\mu_{zz}}{\mu_{3d}} > 1, \qquad (39)$$

because the phonon is more confined. When L_w becomes higher than 45 Å, the mobility rapidly decreases, due to reducing phonon scattering rates in the miniband.

4. Conclusion

In conclusion, the new analytic wavefunction is associated to electron in conduction minibands. We evaluated the expressions of the longitudinal and transverse mobility. The dependences of the relaxation time on the total energy of electron miniband is studied with or without the effect nonparabolicity band. The effect is small for the small energies. We show that electron mobility decreases exponentially with the well width in the superlattice under condition of scattering electron – confined LO-phonon.

References

1. M.V. Klein // *IEEE J. Quantum Electron.* **22**, p. 1760 (1986).
2. M. Cardona // *Superlatt. Microstruct.* **527** (1989).
3. M.C. Thatan, J.F. Ryan and C.T. Foxon // *Phys. Rev. Lett.* **63**, p. 1637 (1989).
4. K. Huang and B.F. Fen // *Phys. Rev.* **B38**, p. 2183 (1988).
5. C. Priester, G. Allan and H. Lannoo // *Phys. Rev.* **B28**, p. 7194 (1983).
6. A. Seilmcier, H.J. Hubner, G.Absteiter, G. Weimann and W. Schlapp // *Ibid.* **59**, p. 1345 (1987).
7. B. Jusserand and M. Cardona, *Light Scattering Solids V*, ed. by M. Cardona.
8. G. Guntherodt, *Topics Apl-Phys.* **66**, p. 49, Springer, Berlin, Heidelberg (1989).
9. M.V. Klein // *IEEE J. Quantum Electron*. **QE-22**, p. 1760 (1986).
10. B. Jusserand, D. Paquet and A. Regreny // *Phys. Rev.* **B30**, p. 6245 (1984).
11. V.M. Fomin and E.P. Pokatilov // *Phys. status solidi (b)* **132**, p. 96 (1985).
12. E.P. Pokatilov, V.M. Fomin and N.N. Semenovskaya // *Phys. Rev.* **B47**, p. 16597 (1993).
13. S. Rudin and T.L. Reinecke // *Ibid.* **B41**, p. 7713 (1990).
14. G. Weker, A.M. de Paula and J.F Ryan // *Semicond. Sci. Technol*. **6**, p. 397 (1991).
15. J. Shi and S Pan // *Phys. Rev.* **B51**, p. 17681 (1995).
16. Gerald Weber // *Ibid.* **B46**, p. 12792 (1993).
17. F.Y. Wu and Chia-Wei Woot // *Chin. J. Phys.* **9**, N 2, p. 68 (1971).
18. H. Rücker, E. Molinari, and P. Lgli // *Phys. Rev.* **B45**, p. 6747 (1992).
19. A.R. Bhatt, K.W. Kim, M.A. Stroscio and J.M Higman // *Ibid.* **B48**, p. 14671 (1993).
20. R. Fuch and K.L Kliewer // *Ibid.* **140A**, p. 2076 (1965).
21. J.J Licari and R. Evrard // *Ibid.* **B15**, p. 2254 (1997).
22. R. Lassmig. // *Ibid.* **B30**, p. 7132 (1984).
23. Xi-Xiq Liang // *J. Phys.* **C4**, p. 9769 (1992).
24. Wenhui Duan, Jia-Lin Zhu and Bing-Lim Gun // *J. Phys. Condens. Matter.* **5**, p. 2859 (1993).
25. R. Ferrira and G. Bastard // *Phys. Rev.*, **B40**, p. 1074 (1989).
26. A. Osted, J Kongsted. K.V Mikkelsen and O. Christiansen // *Molecular Phys.* **101**, N 13, p. 2055, (2003).
27. A.A. Lucas, E. Kartheuser and R.G. Badro // *Phys. Rev.* **B32**, p. 2488 (1970).
28. E.P. Pokatilov and S.I. Beril // *Phys. status solidi (b)* **118**, p. 567 (1983).
29. L. Wendler // *Ibid.* **513** (1985).
30. J.J. Licari and R. Evrard // *Phys. Rev.* **B15**, p. 2254 (1977).
31. K. Huang and B. Zhu // *Ibid.* **B38**, p. 2183 (1988).
32. M. Saitoh // *J. Phys. C: Sol. Stat. Phys.* **5**, p. 914 (1972).
33. G. Weber // *Phys. Rev.* **B46**, p. 16171 (1992).
34. E.O. Kane // *J. Phys. Chem. Solids*, **1249** (1957).
35. A. Person and R.M. Cohen // *Phys. Rev.* **B35**, p. 5568 (1988).
36. U. Ekenberg, *19th Intern. Conf. on the Physics of semiconductors*, Vol. **1**, Warsaw, Poland. Ed. by W. Zawadzki (1988).
37. T. Ando // *J. Phys. Soc. Jpn.* **47**, p. 1518 (1979).
38. T. Ando // *Ibid.* **51**, p. 3900 (1982).
39. P. Vasilopouos and D. Ait el Habti // *Solid State Communs* **71**, p. 675 (1989).
40. G. Bastard // *Phys. Rev.* **B24**, p. 5693 (1981).
41. G. Bastard and J.A. Brum // *IEEE J. Quantum Electron.* **QE-22**, p. 1625 (1986).
42. D. Ait el Habti, P. Vasilopouos and J.F. Curie // *Can. J.* **68**, p. 268 (1990).